

## Accelerated 3D UTE Relaxometry for Quantification of Iron-Oxide Labeled Cells

Bo Zhao<sup>1,2</sup>, T. Kevin Hitchens<sup>3,4</sup>, Anthony G Christodoulou<sup>1,2</sup>, Fan Lam<sup>1,2</sup>, Yijun L. Wu<sup>3,4</sup>, Chien Ho<sup>3,4</sup>, and Zhi-Pei Liang<sup>1,2</sup>

<sup>1</sup>Department of Electrical and Computer Engineering, University of Illinois at Urbana-Champaign, Urbana, IL, United States, <sup>2</sup>Beckman Institute, University of Illinois at Urbana-Champaign, Urbana, IL, United States, <sup>3</sup>Pittsburgh NMR Center for Biomedical Research, Carnegie Mellon University, Pittsburgh, PA, United States, <sup>4</sup>Department of Biological Sciences, Carnegie Mellon University, Pittsburgh, PA, United States

**Introduction:** 3D ultra-short echo time (UTE) relaxometry is a powerful tool for characterizing the biophysical property of tissues with extremely short  $T_2$  or  $T_2^*$  relaxation times (e.g., on the order of hundreds of microseconds) [1]. It enables a wide range of exciting applications (e.g., quantitative tracking of iron-oxide labeled cells) [2]. However, its practical utility has been limited by very long data acquisition times. Recently, various constrained reconstruction methods, e.g., based on sparsity [3] or partial separability (PS) constraints [4], have been developed to enable parameter mapping from undersampled data (e.g., see [5]-[9]). In this work, we use an advanced compressed sensing method [9] based on jointly enforcing PS and sparsity constraints [10] to accelerate 3D UTE relaxometry. The performance of the proposed method is illustrated in a 3D UTE  $T_1$  mapping experiment.

**Method:** We first reconstruct the image sequence  $\rho$  (with variable contrast-weightings) from highly undersampled data  $\mathbf{d}$  using joint PS and sparsity constraints [9]:

$$\hat{\rho} = \arg \min_{\rho} \sum_{\alpha} \sum_{\mathbf{r}} u_{\ell}(\mathbf{r}) v_{\ell}(\alpha) \|\mathbf{d} - \mathbf{E}\rho\|_2^2 + \lambda \sum_{\ell=1}^L \text{TV}(u_{\ell}(\mathbf{r})),$$

where  $\rho(\mathbf{r}, \alpha) = \sum_{\ell=1}^L u_{\ell}(\mathbf{r}) v_{\ell}(\alpha)$  enforces the PS constraint,  $\text{TV}(u_{\ell}(\mathbf{r}))$  represents the total variation regularization which enforces the spatial smoothness constraint on the spatial coefficients, and  $\lambda$  is the regularization parameter. We can estimate  $\{v_{\ell}(\alpha)\}_{\ell=1}^L$  from navigator data using principal component analysis [4]. For example, in variable flip angle UTE  $T_1$  mapping experiments, a set of spokes at the same  $\mathbf{k}$ -space locations can be acquired as navigator data. With the predetermined  $\{v_{\ell}(\alpha)\}_{\ell=1}^L$ , the image sequence  $\hat{\rho}$  can be efficiently determined by additive half-quadratic regularization with a continuation procedure [10]. Following the image reconstruction, the desired parameter maps can be estimated by solving a standard nonlinear least squares problem.

The proposed method was applied to detect iron-oxide labeled cell accumulation in an excised rat heart that experienced an ischemic reperfusion injury. A Brown Norway rat was exposed to a 45-min transient left coronary artery ligation. Following reperfusion, an injection of micro-sized iron-oxide (MPIO) particles (6 mg Fe/kg) was given to systematically label macrophages. At 2 days post injury, the heart was perfused and excised for imaging. Labeled macrophage accumulation at the injury site results in a reduction in tissue  $T_1$  and  $T_2^*$ . The ex-vivo heart was imaged on a 7T Bruker scanner with a variable flip angle 3D UTE sequence with:  $T_E = 20 \mu\text{s}$ ,  $T_R = 10 \text{ms}$ ,  $\text{FOV} = 20 \times 20 \times 40 \text{mm}^3$ , acquisition matrix size =  $200 \times 200 \times 200$ , and spatial resolution of  $0.1 \times 0.1 \times 0.2 \text{mm}^3$ . A total number of 12 flip angles were used, ranging from  $2^\circ$  to  $35^\circ$  with  $3^\circ$  flip angle spacing. To satisfy the Nyquist rate, 125524 half spokes need to be acquired at each flip angle, taking around 21 minutes per flip angle. We performed retrospective undersampling of the above fully acquired data to evaluate the performance of the proposed method. Specifically, we accelerated the acquisition for the first flip angle at a factor of 2 (i.e., acquiring 62762 spokes), while we accelerated the acquisition for the remaining flip angles at a factor of 8.3. The overall acceleration is 6.6. For each flip angle, we acquired 100 spokes at the same set of  $\mathbf{k}$ -space locations that are used as navigator data.

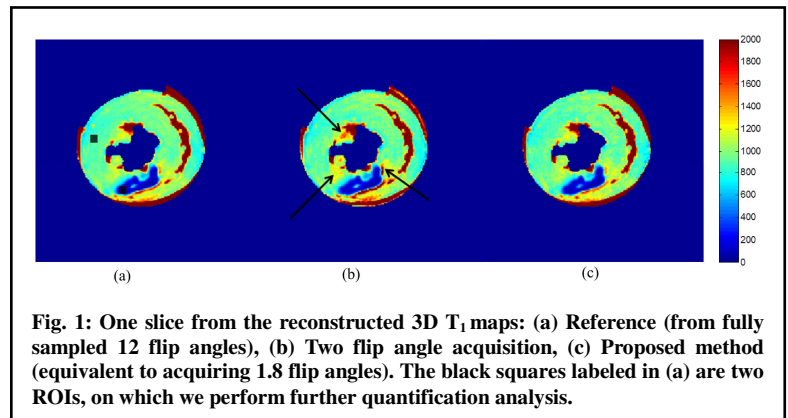


**Fig. 1: One slice from the reconstructed 3D  $T_1$  maps: (a) Reference (from fully sampled 12 flip angles), (b) Two flip angle acquisition, (c) Proposed method (equivalent to acquiring 1.8 flip angles). The black squares labeled in (a) are two ROIs, on which we perform further quantification analysis.**

ROI	Iron-oxide labeled cells	Other myocardium tissues
Reference	127.68 ms	901.68 ms
Two FA acquisition	138.84 ms	921.40 ms
Proposed	<b>124.20 ms</b>	<b>913.36 ms</b>

**Table 1.  $T_1$  values from two ROIs labeled in Fig. 1 (a).**

ROI	Iron-oxide labeled cells	Other myocardium tissues
Two FA acquisition	-9.52%	-2.19%
Proposed	<b>2.73%</b>	<b>-1.30%</b>

**Table 2. Relative errors of  $T_1$  values from two ROIs.**

iron-oxide labeled cell where it is critical for performing quantitative cell tracking.

**Conclusion:** We presented a new model-based reconstruction method for accelerating 3D UTE parametric mapping. We evaluated its performance in a 3D UTE  $T_1$  mapping experiment. Accurate parameter maps have been obtained from highly undersampled experimental data. The proposed method should prove useful for UTE relaxometry and various related biomedical applications (e.g., labeled cell tracking).

**Reference:** [1] Gatehouse *et al.* *Clin Radiol*, 58:1-19, 2003. [2] Liu *et al.* *MRM*, 61:761-766, 2009. [3] Lustig *et al.* *MRM*, 58:1182-1195, 2007. [4] Liang, *ISBI*, 988-991, 2007. [5] Doneva *et al.* *MRM*, 4:1114-1120, 2010. [6] Bilgic *et al.* *MRM*, 66:1601-1615, 2011. [7] Petzschner *et al.* *MRM*, 66:706-716. [8] C. Huang *et al.* *MRM*, 5:1355-1366, 2012. [9] Zhao *et al.* *ISMRM*, p. 2233, 2012. [10] Zhao *et al.* *IEEE TMI*, 1809-1820, 2012. [11] Haldar *et al.* *ISMRM*, p.41, 2007.

**Acknowledgement:** This work is partially supported by the grant NIH-P41 EB001977.